Journal of the Meteorological Society of Japan, Vol. 90, No. 6, pp. 947–958, 2012
DOI: 10.2151/jmsj.2012-606

Low Cloud Modulation by Synoptic Waves over the Eastern Tropical Pacific

Tatsuya TERAO

Graduate School of Environmental Science, Hokkaido University, Sapporo, Japan

and

Takeshi HORINOUCHI

Graduate School of Environmental Science, Hokkaido University, Sapporo, Japan
Faculty of Environmental Earth Science, Hokkaido University, Sapporo, Japan

(Manuscript received 12 April 2012, in final form 29 August 2012)

Abstract

The relation between the synoptic variability of low cloud amounts and the wave disturbances over the eastern tropical Pacific is studied using data from an atmospheric reanalysis (ERA-Interim) and the International Satellite Cloud Climatology Project (ISCCP) over 12 years (from 1990 to 2001). Here, low clouds are defined as those having the tops between 800 and 680 hPa. A significant correlation is found between the low cloud amount and the meridional wind over 3–7 day periods. Composite analyses show that mixed Rossby-gravity waves in the tropics and Rossby waves in mid-latitudes contribute to the synoptic variability of the low cloud amount. These waves induce the fluctuations of the low cloud amount independently, and the low cloud variability is explained as their superposition. Quantitative analyses suggest that these waves affect the low cloud amount through horizontal advection of clouds and the modulation of static stability.

1. Introduction

It has been recognized that clouds play important roles in the global climate and the meteorology. Clouds have a cooling effect by reflecting solar radiation, reducing the incident energy to the Earth's surface, while they have a warming effect by trapping the outgoing infrared radiation. Whether a given cloud has a net cooling or warming effect depends on altitude, optical thickness, and other factors. Therefore, it is important to understand the cloud variability.

Studies on low cloud variability have been conducted on the subtropical regions (e.g., offshore California or Peru) where the amount of low stratiform clouds is climatologically large. These regions are located under the subsidence in the descending branch of the Hadley circulation. Using data from surface-based observations, Klein and Hartmann (1993) (hereafter, KH93) studied the low cloud seasonal cycle over ten regions where the low cloud amount is large. They showed that a linear relationship exists between the lower tropospheric static stability and the seasonal mean low cloud amount. Here, the stability was defined as the difference in potential temperature between 700 hPa and the surface, and it is used as a measure of the trade inversion. The slope of the relation is 6% K^{-1}.

Wylie et al. (1989) studied the synoptic variability of the low cloud amount over the subtropical northeastern Pacific from an observation over 21 days. They found that the low cloud variability is related to temperature

Corresponding author and present affiliation: Tatsuya Terao, New Chitose Aviation Weather Station, Japan Meteorological Agency in New Chitose Airport Terminal, Bibi, Chitose-shi, Hokkaido 066-0012, Japan
E-mail: t-terao@met.kishou.go.jp

advection in the planetary boundary layer, 500 hPa height, and boundary layer depth. Klein (1997) also studied the synoptic variability of the low clouds using a long data record at an ocean weather station (30°N, 140°W). They found that the low cloud variability with synoptic time scale is strongly correlated with the lower tropospheric stability, as it is for a month or longer time scale. Furthermore, it was shown that the strength of the subtropical high is associated with the increase in the low cloud amount. Rozendaal and Rossow (2003) studied the intraseasonal variability of the low clouds in the subtropical regions using data from the International Satellite Cloud Climatology Project and the European Center for Medium-Range Weather Forecasts reanalysis, and they suggested a relation between synoptic-scale waves and the low cloud variability.

Xu et al. (2005) studied the subseasonal variability of the low clouds with a time scale shorter than the seasonal cycle over the subtropical southeastern Pacific using satellite data, buoy observation data, and the National Centers for Environmental Prediction and the National Center for Atmospheric Research (NCEP-NCAR) reanalysis. They used the column-integrated cloud liquid water (CLW) as a measure of the clouds. They found that an increase in CLW is correlated with an anomalous anticyclonic circulation (enhanced subtropical high). They suggested that the cold advection in the boundary layer, together with an enhanced warming associated with the subsidence in anticyclonic circulation, acts to intensify the lower tropospheric stability to increase the low cloud amount. These studies have elucidated the contribution of subtropical and mid-latitudinal wave disturbances to the synoptic variability of the low clouds.

In the deep tropics, synoptic wave disturbances are also present, such as barotropic instability waves, mixed Rossby-gravity waves and tropical depression type disturbances. The barotropic instability waves, such as African waves are present in the tropical easterly zone (e.g., the Atlantic Ocean, the Pacific Ocean). Their features have been studied through observation (e.g., Burpee 1974; Serra and Houze 2002; Petersen et al. 2003). The Pacific easterly waves have a wavelength of 4200-5900 km and the a period of about 3-6 days (Serra et al. 2008). Their axis is oriented southwest-northeast between 0° and 20°N in the eastern Pacific, and they are coupled with the deep convection in the Intertropical Convergence Zone (ITCZ).

The mixed Rossby-gravity (hereafter, MRG) waves are equatorially trapped (Matsuno 1966), and were observationally found by Yanai and Maruyama (1966). It is known that the MRG waves are often coupled with deep convection in the ITCZ (Liebmann and Hendon 1990; Takayabu and Nitta 1993; Wheeler and Kiladis 1999). Yokoyama and Takayabu (2012) studied the relationship between the rain systems, synoptic-scale disturbances, and large scale environment over the eastern tropical Pacific. They found that the deep convective systems in the ITCZ are frequently associ ated with the disturbances in which low-level vortices and MRG waves are coupled.

The studies mentioned above have shown the relation between equatorial wave disturbances and deep convective activity in the ITCZ. In this study, we focus on the relation between the equatorial disturbances and low cloud variability in the eastern tropical Pacific (240–280°E, 5°N–20°S). The climatological low cloud amount in this region is high, but the relationship between the low cloud amount and synoptic-scale disturbances on a several day time scale has not been studied much. In this study, we elucidate their relationship and its causes.

The rest of the paper is organized as follows. Section 2 describes the datasets and the analytical methods used in this study. Section 3 shows the results. Conclusions are drawn in Section 4.

2. Data and methods

2.1 Data

The data used in this study are the European Center for Medium-Range Weather Forecasts (ECMWF) Reanalysis (hereafter, ERA-Interim), the International Satellite Cloud Climatology Project (ISCCP) D1 cloud data (hereafter, ISCCP-D1), and D2 cloud data (hereafter, ISCCP-D2). Analyses are conducted for boreal falls (August-December) over 12 years (1990–2001) except for a power spectral analysis (see Subsection 2.2).

The ERA-Interim is 6-hourly atmospheric data with a horizontal resolution of 1.5° × 1.5°. Zonal wind, meridional wind, vertical p-velocity and temperature are used in the analyses. The ISCCP-D1 is 3-hourly cloud data with a horizontal resolution of 2.5° × 2.5° created by combining data from geostationary and polar-orbiting satellites. We used the cloud amount data derived from infrared (IR, 11 μm wavelength) channels. The cloud amount is classified according to the cloud top pressures (the low clouds: 1000–800 hPa and 800-680 hPa, the middle clouds: 680–560 hPa and 560–440 hPa, the high clouds: 440–310 hPa, 310–180 hPa and 180–10 hPa). The sum of the cloud amount of all the seven layers is less than or equal to 100%.

In the satellite infrared observation, lower clouds

are hidden by upper clouds. However, the middle and high cloud amount is climatologically small (about less than 20%) in the southern hemispheric tropical eastern Pacific (Fig. 1a). In this study, we use the cloud amount of the second-level (800–680 hPa). We did not use the first level (1000–800 hPa) since the second-level cloud amount is high (about 20–70%, see Fig. 1b). In this study, we use the following corrected low cloud amount (CLCA) as the measure of the low cloud amount:

$$\mathrm{CLCA}[\%] = \frac{\text{the second layer's cloud amount }[\%]}{100 - \text{the middle and high cloud amount }[\%]} \times 100 \quad (1)$$

where the middle and high cloud amount in Eq. (1) is the sum of the cloud amount from the third to the seventh layer. The CLCA is set to be missing when the middle and high cloud amount is greater than 50%. We checked the sensitivity of our results to this threshold percentage and found that changing it has only small impacts.

We also used the ISCCP-D2 data, which are monthly mean data derived from the D1 data, in order to study some climatological features. The parameters used in this study are the cloud amounts for each of the cloud types: stratus, cumulus, and stratocumulus for low clouds. Here, unlike in the ISCCP-D1, the low clouds are not subdivided into the two levels (800–680 hPa and 1000–800 hPa). The cloud type specification is made in terms of the optical thickness.

2.2 Methods

We conduct power spectral analyses to find the dominant time scales and cross spectral analyses to elucidate the relation between two given quantities. These spectral analyses are conducted using 12-hourly CLCA obtained by binning the 3-hourly CLCA.

In the power spectral analyses, the power spectrum density (PSD) is obtained by the Fourier transform auto-correlation function obtained from a value time sequence over the full 12 years. In the cross spectral analyses, the co- and quad-spectra are computed from the Fourier transform of the cross-correlation function for each boreal fall. Then, the co- and quad-spectra are ensemble-averaged over the 12 seasons. Finally, the coherence squared and phase are obtained from the spectra.

We conduct composite analyses to elucidate spatial features of disturbances having the periods over 3–7 days and further investigate the mechanisms of low cloud variability. In a composite analysis, a reference

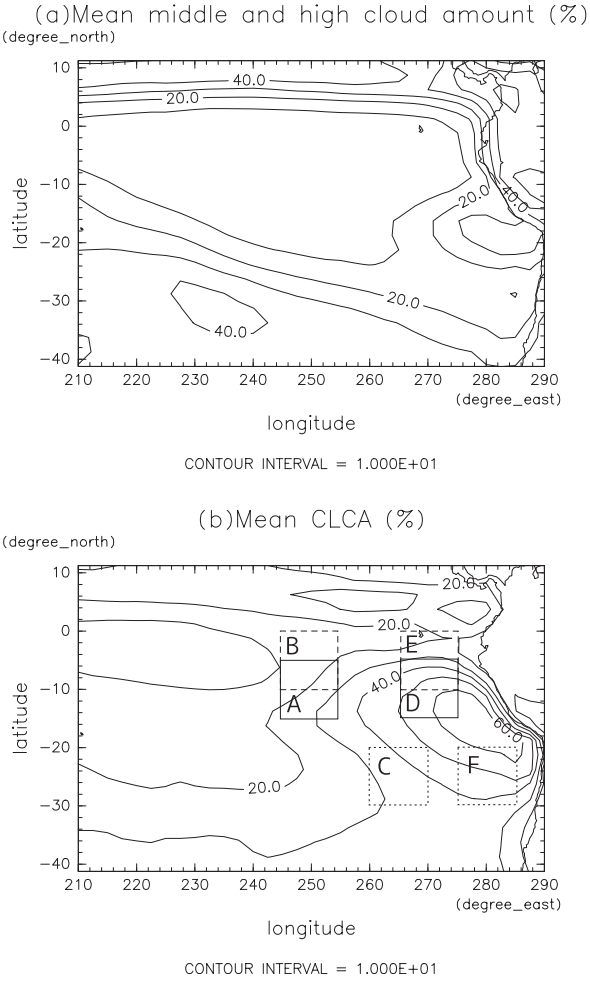

Fig. 1. Mean cloud amount distribution (%) of (a) the middle and high cloud (680–10 hPa) and (b) CLCA (800-680 hPa). The boxes in Fig. 1b are the domains used to average CLCA (box A: 245–255°E, 5–15°S, D: 265–275°E, 5–15°S) and the meridional wind (box B: 245–255°E, 0–10°S, C: 260–270°E, 20–30°S, E: 265–275°E, 0–10°S, F: 275–285°E, 20–30°S) in the spectral analyses (section 3.1) and the composite analyses (section 3.2 and 3.3).

time series is obtained by averaging a key quantity (such as CLCA or the meridional wind) over a horizontal box whose longitudinal and latitudinal sizes are 10°. A 3–7 day band-pass filter is applied to the reference time series, and its standard deviation is computed. Here, the filtering is made with running means; 7-day running means are subtracted from 3-day running means. Note that the period at which the amplitude is halved by running means is 1.66 times the

duration of the means. A positive (negative) composite is made over periods at which the band-passed reference value is greater than +1 standard deviation (less than −1 standard deviation). In many cases, the object of the composite analysis is also band-passed with the same filter. In this case, we call the composite as the composite *anomaly*.

A statistical significance test of the CLCA composite anomaly is made using the Student's t-test. Here, the degree of freedom is set to be the number of days divided by 2, which is the assumed correlation time scale in the reference is 2 days.

In Subsection 3.2.b, 3.2.c and 3.3, we examine the following three effects as possible causes of the low cloud amount variability: 1) horizontal advection of clouds, 2) lower tropospheric stability, and 3) vertical advection of humidity. Their impacts are estimated as follows.

The effect 1) is estimated from the composite anomaly of the horizontal wind at 700 hPa and the composite of CLCA by the following equation.

$$\Delta C = -\upsilon' \cdot \nabla_H C^* \cdot \Omega^{-1} \tag{2}$$

where ΔC is the estimated increment of CLCA by horizontal advection, υ' is the composite anomaly of the horizontal wind, $\nabla_H C^*$ is the horizontal gradient of the composited CLCA, $\Omega^{-1} = T/2\pi$, and T =5 days representing the periods of the disturbances investigated in this study.

The effect 2) is derived from the composite anomaly of the lower tropospheric stability by assuming the KH93 relation.

$$\Delta C = kS' \tag{3}$$

where k=6% K^{-1} and S' is the composite anomaly of the lower tropospheric stability defined as the difference in the potential temperature between 700 and 1000 hPa. This formula is derived from seasonal anomalies. Therefore it is likely an overestimate to apply it to the transient disturbances on the order of a few days since the time scale is shorter than that needed to replenish the boundary layer humidity. Assuming a typical climatological evaporation rate in the tropical eastern Pacific, the time scale to supply a climatological column water vapor amount between 1000 and 700 hPa is estimated to be about 20 days.

Since it is difficult to quantitatively relate the fluctuations in vertical wind and cloud amount, the effect 3) is evaluated only indirectly. The composite anomaly of the vertical water vapor flux $(\omega q)'$ can be approximated by $\omega'\overline{q}$, where ω is the vertical p-velocity, q is specific humidity, prime mark and over-bars represent an anomaly and climatological means, respectively. This is because $O(\omega') \gg O(\overline{\omega})$ and $O(q') \ll O(\overline{q})$. Therefore, we estimate the effect of ω' on relative humidity. Here, it is made by the vertical motion of near saturated air masses. Suppose the vertical displacement of an initially saturated air parcel is at 700 hPa, the relative humidity change is defined as

$$\Delta RH = \frac{q^*(p,\ \theta)}{q^*(p+\Delta p,\ \theta)} - 1 \tag{4}$$

where q^* is the saturation specific humidity, p = 700 hPa, and θ is the potential temperature at 700 hPa. The pressure perturbation Δp is derived by assuming a sinusoidal fluctuation with time as, $\Delta p = \Omega^{-1}\omega'$, where ω' is the composite anomaly of the vertical p-velocity ω.

3. Results

3.1 Climatology and Spectral features

Figure 1b shows the mean CLCA (800–680 hPa) distribution in boreal falls (August-December) over 12 seasons. The maximum amount (greater than 60%) lies off the western coast of South America between 10°S and 25°S. The low cloud amount decreases gradually with the distance from this area.

The low cloud amount in Fig. 1b is for all cloud types. The contribution of individual cloud types are examined using the ISCCP-D2 (not shown). Over the eastern tropical and subtropical Pacific, the amount of the stratus, the cumulus, and the stratocumulus clouds are roughly 5% or smaller, 5–15%, and 15–45%, respectively. Note, however, that the percentages are for the total low cloud amount including the first level (1000–800 hPa).

Figure 2 shows the time-longitudinal cross sections of CLCA averaged between 5°S and 15°S, and the meridional wind at 700 hPa averaged between 0° and 10°S. The period, September 2001, overlaps with that of the Eastern Pacific Investigations of Climate (EPIC2001) campaign (Petersen et al. 2003). The meridional wind exhibits a westward-propagating synoptic fluctuation whose time scale is several days. CLCA also has similar but less clear features.

Figure 3 shows the power spectra of CLCA over box A and the meridional wind over box B for the full 12 years (1990–2001) in energy content form. CLCA spectrum is enhanced over a period of 3–20 days, peaking at around 5 days (Fig. 3a). The meridional wind spectrum has a narrower enhancement over a period of 3–7 days, peaking at around 5 days (Fig. 3b). These spectral features are similar at other longitudinal zones over the eastern tropical Pacific.

Figure 4a shows the coherence-squared, a measure

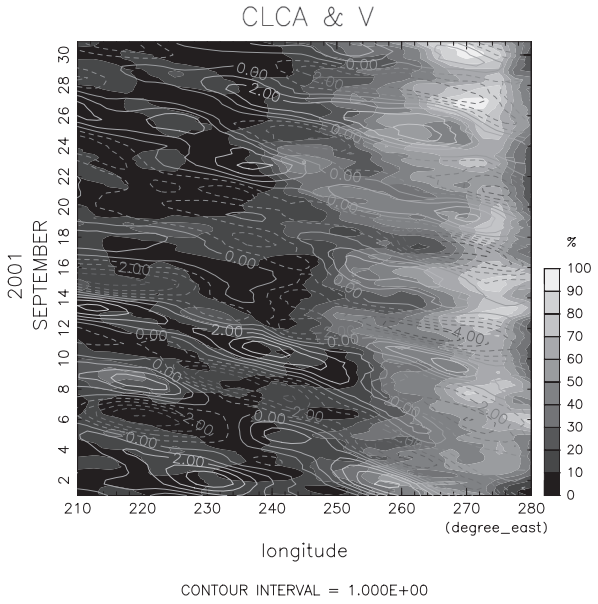

Fig. 2. Time-longitude plot (September 2001) of the 24-h running mean CLCA (shade, %) and the meridional wind at 700 hPa (solid contours: southerly, dashed contours: northerly, m s^{-1}). CLCA is averaged between 5–15°S, and the meridional wind is averaged between 0–10°S.

of cross correlation, between CLCA and the meridional wind averaged over boxes A and B respectively, both of which are in the tropics. Significant correlation is found over a period of 3-10 days, maximizing at a 5 day period. Similar significant correlation is found over the longitudinal band between 240°E and 280°E, although the correlation decreases gradually as the distance from the coast decreases. Here, the domain used to average the meridional wind is situated northward by 5° with respect to that of the low cloud. If the former domain is moved to coincide with the latter, similar significant correlation is found, but the values are lower (not shown). If the former domain is moved to further southward by 5°, the correlation is not significant (not shown).

Figure 4b shows the coherence-squared between CLCA in the tropics (box A) and the meridional wind in the extratropics (box C). The overall coherence over a period of 3–10 days is weaker than Fig. 4a, as one might expect from the greater distance between the boxes used for averaging. However, the peak at the 5 day period is significant.

3.2 The low cloud and waves over the offshore region far from South America

In Subsection 3.1, we showed that the low cloud variability is linked to the variability of the atmospheric dynamical fields on the synoptic time scale. In this section, we investigate the spatial features of 3–7 day disturbances, and the mechanisms to affect the low cloud variability by using composite analyses. First, we focus on the offshore region far from South America (longitudinal range is 240–260°E). The mean low cloud amount in this region is about 20–40% (Fig. 1b).

a. The composites based on the low cloud amount

Figure 5 shows the composite anomalies of CLCA and the horizontal wind at 700 hPa using CLCA averaged over box A as the reference time series. Here, composite is made if the band-passed (3–7 days) CLCA anomaly exceeds the standard deviation (positive composite; see Subsection 2.2). In this paper, we only show the positive composites. Negative composites are not shown because they are close to mirror images of the positive composites.

There is an area of positive anomaly CLCA (about 10%) in box A, and two synoptic scale vortical structures are present in the horizontal wind field both on the north and south sides of box A. The former is the clockwise vortex indicated by the star mark in Fig. 5 whose center is at around 256°E, 2°S, and the latter is a counterclockwise vortex indicated by the filled circle in Fig. 5 whose center is at around 250°E, 32°S. Hereafter, the former is called "the tropical vortex" and the latter is called "the mid-latitude vortex".

The southerly wind peak associated with the tropical vortex exists near 245°E, and the largest positive anomaly of CLCA lies in the southeast of this southerly peak. Since the tropical vortices propagate westward, this relation indicates that the increase in the low cloud amount follows the southerly anomaly. This result is consistent with the phase lag obtained by cross spectral analyses (not shown). Also, this enhancement of CLCA lies in the north of the mid-latitude counterclockwise vortex.

b. Low cloud modulation by the tropical vortices

The composite analysis based on the low cloud amount (section 3.2a) indicated its association with the tropical and the mid-latitude vortices. We now investigate the role and the nature of the tropical vortices by using the composite analyses based on the meridional wind in the tropics.

Figure 6a shows the composite CLCA anomalies

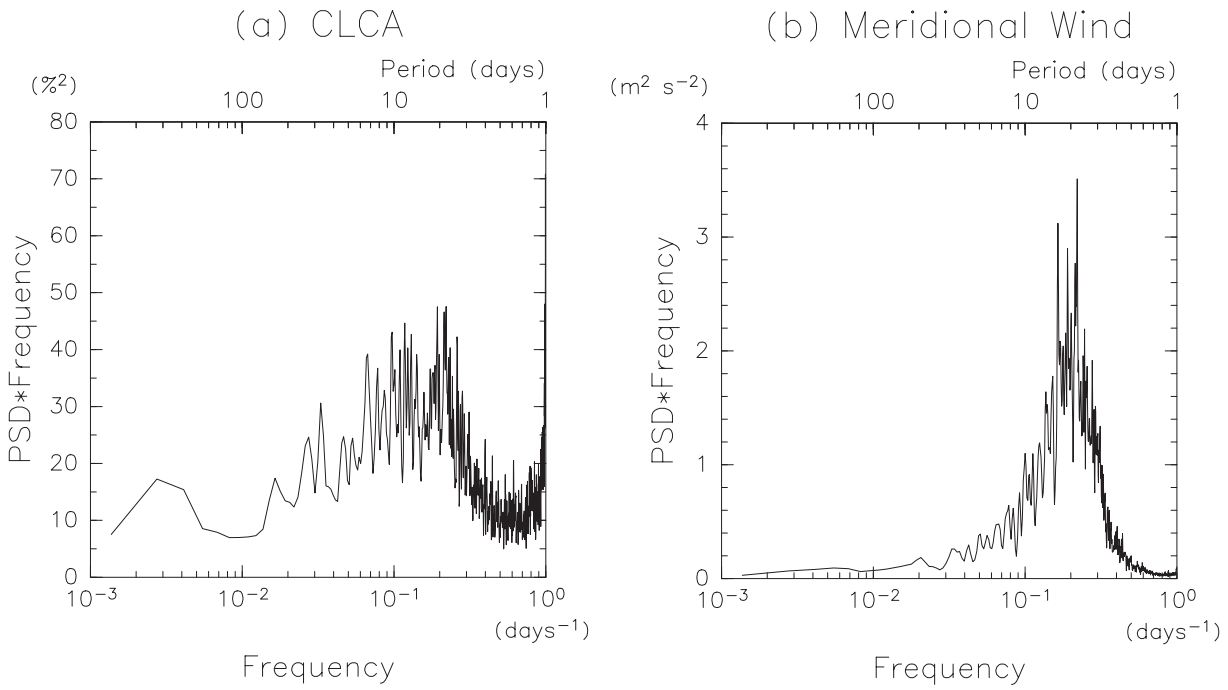

Fig. 3. Power spectra of (a) CLCA ($\%^2$, averaged over the box A in Fig. 1b) and (b) the meridional wind at 700 hPa ($m^2\ s^{-2}$ averaged over the box B in Fig. 1b). The abscissa: log-scaled frequency (cycles per day), the ordinate: linearly-scaled power spectral density (PSD) × frequency (energy-content form).

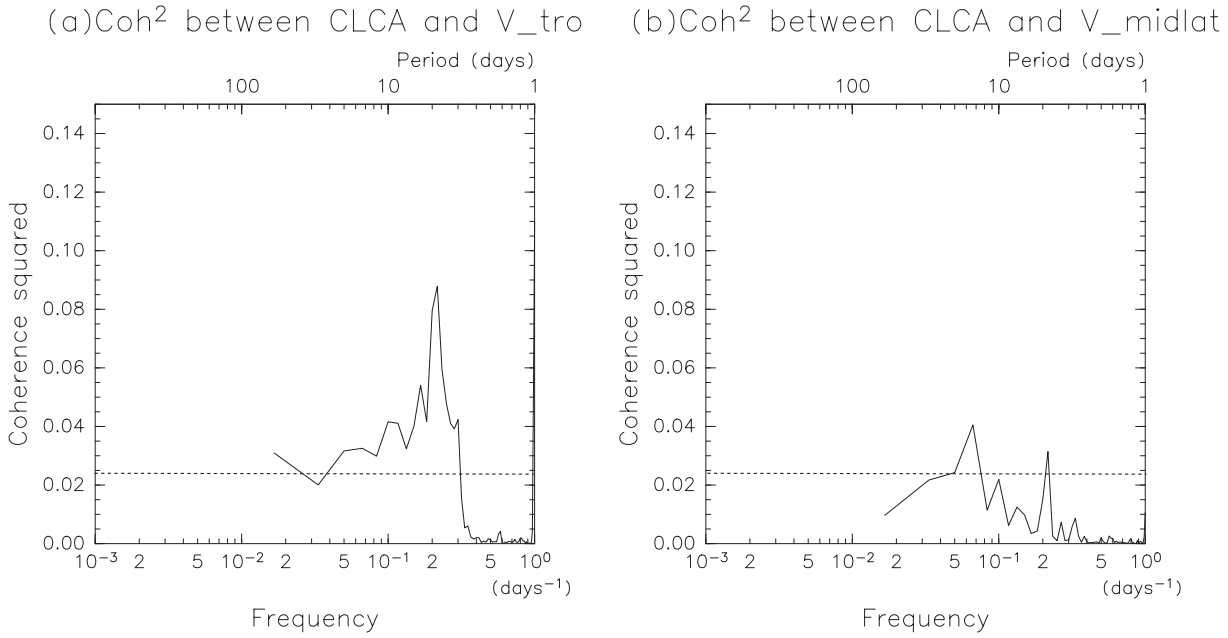

Fig. 4. Coherence squared between CLCA (averaged over the box A in Fig. 1b) and the meridional wind at 700 hPa (a: averaged over the box B in Fig. 1b, b: averaged over the box C in Fig. 1b). The dashed line shows the 95% significance level.

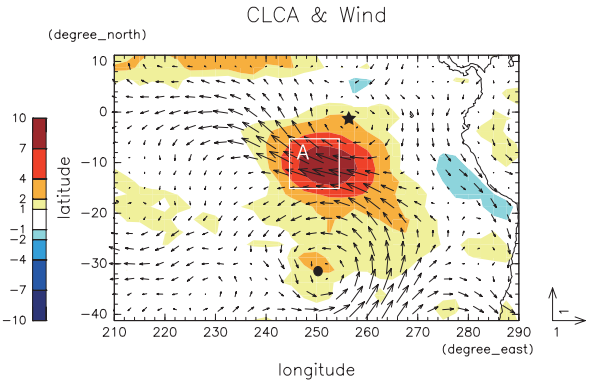

Fig. 5. Composite results by using the 3–7 day band-passed CLCA over the box A (245–255°E, 5–15°S) as the reference time series (positive composite). Arrows show the composite anomalies of 700 hPa horizontal winds (m s^{-1}). Shades show the composite anomaly of CLCA (%). ★ : the center of the tropical vortex, ●: the center of the middle-latitude vortex.

and horizontal wind at 700 hPa. The reference time series is the band-passed (3–7 days) meridional wind averaged over box B (positive composite). The tropical vortex in Fig. 5 is more clearly reproduced in Fig. 6a, which is accompanied by a counterclockwise vortex to the west. Also, there is a statistically significant positive CLCA anomaly (about 1.5–4%) on the southwest side of the clockwise vortex, which almost the entirely covers box A. The positional relationship between the vortex and CLCA anomaly is consistent with that in Fig. 5. The CLCA anomaly in Fig. 6a is smaller than in Fig. 5, but it is because the correlation between the meridional wind and CLCA is not perfect (Fig. 4).

The mid-latitude vortex shown in Fig. 5 is not clear in Fig. 6a. This result indicates that the tropical vortices and the mid-latitude vortices are independent of each other. The tropical vortex has a horizontal scale of about 3500 km in the zonal direction (zonal wavenumber 5–6) and propagates westward. The spatial structure of the tropical vortices is consistent with MRG waves. This interpretation is reinforced as follows. The equivalent depth calculated from the meridional scale of the composited vortex in Fig. 6a is about 10 m if they are MRG waves. The equivalent depth estimated alternatively from the phase speeds in Hovmöller diagrams (such as Fig. 2) and the dispersion relation of MRG waves is about 2–90 m, this large variation is primarily due to the variation in the background mean flow. These estimates are roughly consistent with preceding studies (Takayabu and Nitta 1993; Wheeler and Kiladis 1999).

We examine the following three effects as possible causes of the low cloud variability induced by the tropical vortices: 1) horizontal advection of clouds, 2) lower tropospheric stability, and 3) vertical advection of humidity (see Subsection 2.2).

Figure 6b shows the composite CLCA and the composite anomaly of the horizontal wind at 700 hPa. The wind direction on the southwest side of the clockwise vortex is east-southeasterly to southeasterly. Based on the method introduced in Subsection 2.2, it is estimated that the advection associated with the composite wind anomaly increases the cloud amount in box A by 1.5%. This value is a half of the cloud amount anomaly in Fig. 6a (about 3%).

Figure 6c shows the composite anomaly of the lower tropospheric stability defined as the difference in the potential temperature between 700 hPa and 1000 hPa (KH93). The positive anomaly, about +0.3 K, exists on the west side of the clockwise vortex. It corresponds to the increase in CLCA in box A by 1.8% or smaller. This value is comparable to that due to the horizontal advection, but it is likely an overestimate for the transient disturbances since it is a naïve application of the KH93 relation (Subsection 2.2).

Figure 6d shows the composite anomaly of vertical flow averaged over 925–750 hPa. An area of weak ascent (negative anomaly) exists on the southwest side of the clockwise vortex, which is deviated slightly eastward from the theoretical expectation. The vertical advection can have an impact on the cloud amount, but the anomaly peak in the composite is located a little in the east to explain the low cloud anomaly from this point of view. The estimated impact on the relative humidity in the box A is 2.1%. A further quantitative estimation on its impact on the CLCA is not available.

Table 1 summarizes the quantitative estimates of the two mechanisms. It is suggested that the horizontal advection and the stability effects are important for the low cloud amount variability. Figure 7 shows the longitude-pressure cross section of the composite anomaly of the vertical p-velocity averaged over 5–15°S. The vertical structure of the vertical p-velocity is tilted eastward with altitude in the lower to middle troposphere, which is consistent with the typical boomerang shape of the MRG waves (e.g., Wheeler et al. 2000). Over box A (245–255°E), the vertical advection is ascent and descent below and above 700hPa, respectively. At 700 hPa, it is descent in the west of box A. Since the waves propagate westward, this feature is consistent with the positive anomaly in the lower tropospheric

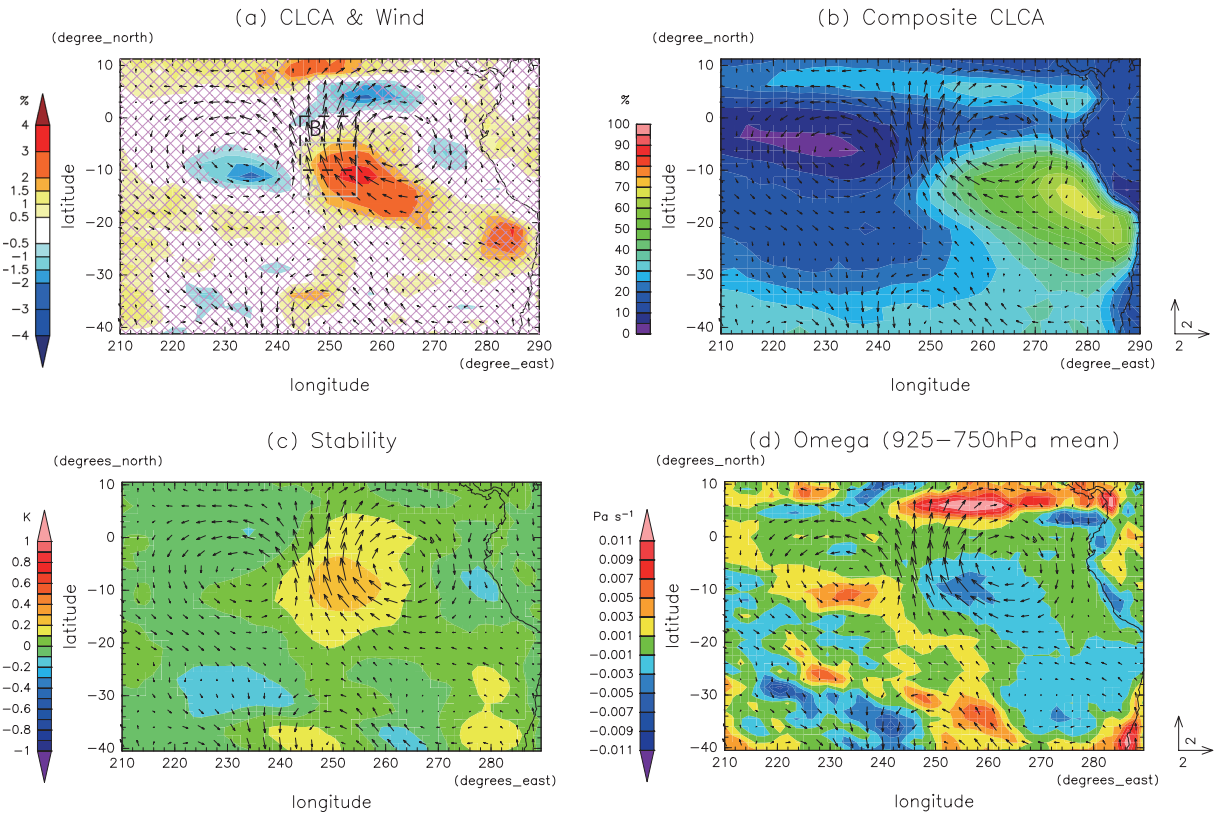

Fig. 6. Composite results by using the 3–7 day band-passed meridional wind over the box B (245–255°E, 0–10°S) as the reference time series (positive composite). Arrows show the composite anomalies of 700 hPa horizontal winds (m s^{-1}, all panels). Shades show the composite anomalies of (a) CLCA (%), (c) the lower tropospheric stability (K), and (d) the vertical p-velocity averaged over 925–750 hPa (Pa s^{-1}). Shades in the panel (b) is the composite CLCA without subtracting the mean, i.e., not an anomaly, (%). Cross-hatching in the panel (a) denotes areas where CLCA composite anomaly is not significant at the 95 percent level.

Table 1. CLCA anomalies in the box A and the estimates of the contribution from the horizontal advection and stability modulation obtained from the composite analyses by using the band-passed 700 hPa meridional wind as the reference time series.

	the tropical vortices (Fig. 6)	the mid-latitude vortices (Fig. 8)
composite CLCA anomaly	1–4%	1–2%
horizontal advection	1.5%	0.9%
lower tropospheric stability	≤ 1.8%	≤ 1.2–1.8%

stability around box A as shown in Fig. 6c. Composite anomaly of the mid and high cloud amounts are not computed in this study. However, the vertical wind anomaly over box A has a suppression effect on deep convection, since the vertical wind anomaly over box A is downward above 700 hPa.

c. Low cloud modulation by the mid-latitude vortices

Figure 8 shows the composite fields as in Fig. 6, but the region used to derive the reference time series is taken in mid-latitude (box C). A mid-latitude vortex train similar to the vortex in Fig. 5 is obtained, which is likely Rossby waves. There is an area of statistically significant positive CLCA anomaly in the counter-clockwise vortex whose center is 258°E, 36°S, which

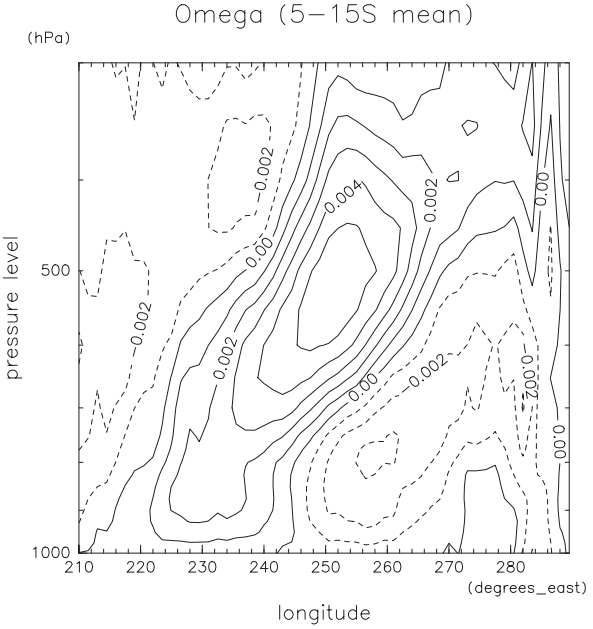

Fig. 7. Composite result as in Fig. 6, but the composite quantity is the composite anomaly of the vertical p-velocity (Pa s^{-1}) averaged between 5–15°S (Longitude-pressure cross section). The box A is located on the center of the region (245–255°E).

extends equatorward up to 10°S. In box A, the anomaly is partially significant. This result is roughly consistent with the result of the cross spectrum analysis (Fig. 4b), where the coherence-squared is partially significant in periods of 3 to 7 days. The positional relationship between the mid-latitude vortex and the area of positive CLCA anomaly in the tropics is consistent with Fig. 5.

We assessed the three effects (horizontal advection, stability, and vertical advection effect; see Sub-subsection 3.2.b) from Fig. 8. The effect of the horizontal advection is estimated to be 0.9% in box A. Also, there is good correspondence between the CLCA anomaly and the stability anomaly (Fig. 8c). The positive stability anomaly associated with the counterclockwise vortex is about +0.2-0.3 K in box A, corresponding to CLCA increase by 1.2–1.8% if it is based on the KH93 relation. The vertical advection is unimportant since the area of positive CLCA anomaly and the vertical flow anomaly do not coincide around box A (Fig. 8d).

Based on the above estimation of the three effects, it is suggested that mid-latitude vortices contribute to the low cloud amount variability through stability and horizontal advection effects.

We also examined the vertical structure of the mid-latitude vortices (not shown). It is roughly barotropic over the troposphere.

d. Combined effects from the equatorial and mid-latitude vortices

The results of the composite analyses in Sub-subsection 3.2.b and 3.2.c show that both the tropical vortices and the mid-latitude vortices can contribute to the low cloud variability. The magnitude of the low cloud anomaly in a 3–7 day time scale is largely determined by influence superposition by the tropical and mid-latitude vortices, which are independent. Figure 9 is a schematic diagram to show the relation between the low cloud anomaly and wave disturbances. The low cloud amount in the tropics is affected by both the tropical and mid-latitude vortices.

3.3 The low cloud and waves over the coastal region of South America

In the previous section, the relation between the low cloud variability and the atmospheric dynamical fields is investigated over the offshore region far from South America. In this section, we focus on the near-coastal region (longitudinal range is 260–280°E) of South America. The mean low cloud amount in this region is about 40–60% (Fig. 1b).

Figure 10a shows composite CLCA anomalies and horizontal wind at 700 hPa using CLCA averaged over box D in the tropics as a time series reference. There is an area of positive CLCA anomaly (about 10%) in box D, and southeasterly flow is present along the west coast of South America between 0° and 20°S. This positional relationship is similar to that in Fig. 5. However, a distinction between the tropical vortex and the mid-latitude vortex is unclear compared with Fig. 5.

Figure 10b shows the composite anomalies as in Fig. 10a, but the reference time series is the meridional wind averaged over box E. An area of statistically significant positive CLCA anomaly, exists around box E. The southeasterly flow along the west coast of South America is similar to that of Fig. 10a. A counterclockwise vortex whose center is at 254°E, 7°S is present over the ocean, but the clockwise vortex to its east is not closed flow over the continent is obscure. Even so, the positional relationship between the counterclockwise vortex and the area of positive CLCA anomaly is consistent with Fig. 6a. The quantitative assessments of the three effects (horizontal advection of clouds, stability and vertical advection of humidity) are as follows: the horizontal advection can increase

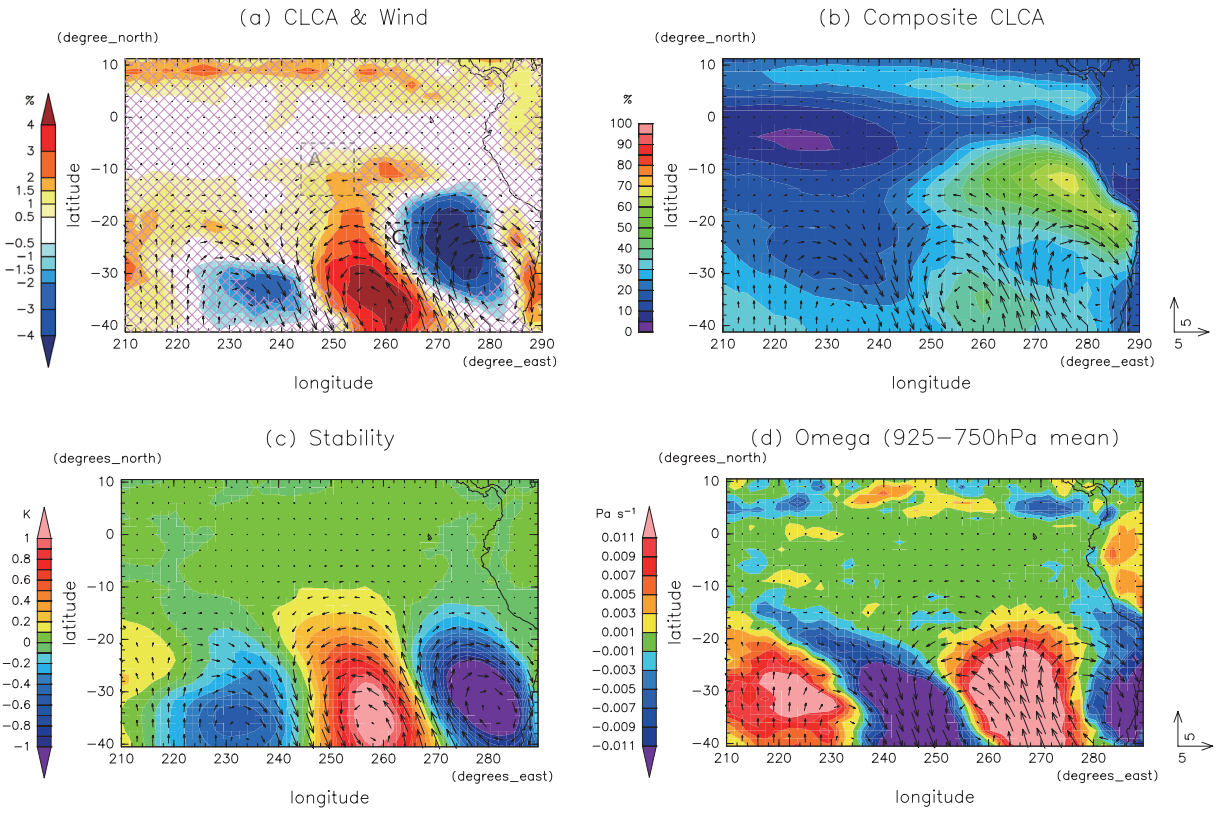

Fig. 8. As in Fig. 6 but for the composite results by using the 3–7 day band-passed meridional wind over the box C (260–270°E, 20–30°S) as the reference time series.

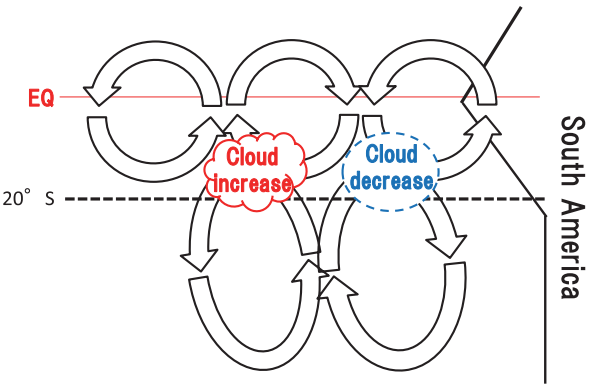

Fig. 9. Schematic diagram to show the relation between the low cloud amount anomalies and the wave disturbances. The solid arrows: the horizontal wind at 700 hPa, the upper vortices: the tropical vortices (MRG waves), the lower vortices: the mid-latitude vortices (Rossby waves), and the red horizontal line: the equator.

the low cloud amount by 3%, the stability effect can increase it by 2.4% or smaller, and the vertical advection can qualitatively increase the low cloud amount by increasing the relative humidity through upwelling (its effect is estimated to be about 2%).

Figure 10c shows the composite anomalies as in Fig. 10a, but the reference time series is the meridional wind averaged over box F in the subtropics. A mid-latitude counterclockwise vortex exists offshore of South America. An area of highly positive CLCA anomaly is present on the north side of the vortex which continues to box D in the tropics, although it is weak (about 2%). The positional relationship between the mid-latitude vortex and the area of positive CLCA anomaly around box D is consistent with Fig. 8a. The quantitative assessments of the three effects are as follows: the horizontal advection effect is about 1.7%, the stability effect is 2.4% or smaller, and the vertical advection is unimportant.

Xu et al. (2005) showed the relation between the low cloud anomaly and the subtropical disturbance over the

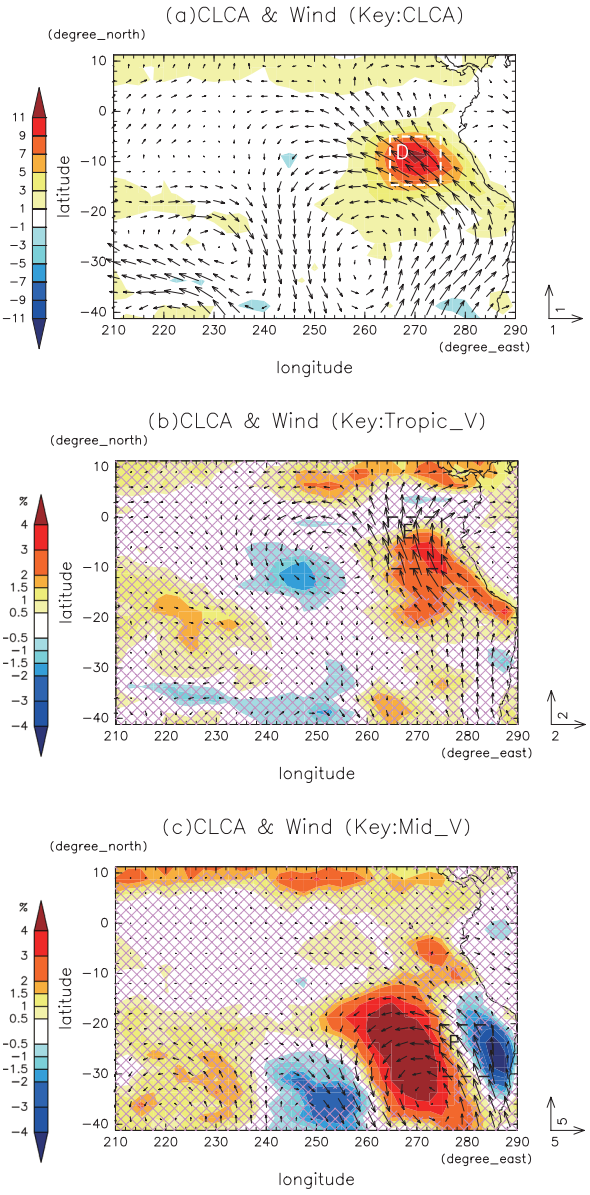

Fig. 10. Composite results for near-coastal region. Each panel shows the composite (a) based on CLCA (box D), (b) based on the meridional wind in the tropics (box E) and (c) based on the meridional wind in the subtropics (box F). Arrows show composite anomalies of 700 hPa horizontal winds (m s^{-1}). Shades show composite anomalies of CLCA (%). Cross-hatching in the panel (b) and (c) denotes areas where CLCA composite anomaly is not significant at the 95 percent level.

near-coastal region of South America. Our composite result (Fig. 10c) is similar to their positional relationship between the low clouds and the disturbance, although the time scale they examined, which is sub-seasonal, is longer than that examined in the current study. They attributed it to the lower tropospheric stability associated with disturbances that contribute to an increase in low clouds. The current study suggested that this reasoning holds on shorter time scales too.

4. Conclusions

We have elucidated the relation between the low cloud variability and the atmospheric wave disturbances over the tropical eastern Pacific. Both the low cloud and the meridional wind at 700 hPa have westward-propagating periodic fluctuations. The dominant time scale of the low cloud fluctuation is 3–20 days, and that of the meridional wind is 3–7 days. These fluctuations are significantly correlated.

The composite analyses conducted for the offshore region (240°–260°E) show the existence of tropical and mid-latitude vortices, which contribute to the synoptic variability of the low cloud amount on a 3–7 day period. The tropical vortices are mixed Rossby-gravity waves, and the mid-latitude vortices are Rossby waves. These waves are independent, and the low cloud variability in a several day period is explained as the superposition of the modulations induced by these waves.

Quantitative estimation of the possible causes of synoptic variability of low cloud values suggests that the horizontal advection of clouds and the stability effect are important in low cloud modulation by the tropical vortices. These effects are also important in the low cloud modulation by mid-latitude vortices.

The low cloud amount variability over the near-coastal region of South America is explained similarly. However, the tropical and mid-latitude vortices are less separable.

Acknowledgements

The authors would like to thank Youichi Tanimoto, Atsushi Kubokawa and Fumio Hasebe for their helpful comments and discussion. We also thank two anonymous reviewers for constructive comments on earlier versions of this paper and Masaru Inatsu, the editor in charge, for helpful advice. This study is partially supported by the JSPS grant-in-aid 22540444. Analyses are made by using the GFD Dennou Ruby library.

References

Burpee, R. W., 1974: Characteristics of north african easterly waves during the summer of 1968 and 1969. *J. Atmos.*

Sci., **31**, 1556–1570.

Klein, S. A., 1997: Synoptic variability of low-cloud properties and meteorological parameters in the subtropical trade wind boundary layer. *J. Climate*, **10**, 2018–2039.

Klein, S. A., and D. L. Hartmann, 1993: The seasonal cycle of low stratiform clouds. *J. Climate*, **6**, 1587–1606.

Liebmann, B., and H. H. Hendon, 1990: Synoptic-scale disturbances near the equator. *J. Atmos. Sci.*, **47**, 1463–1479.

Matsuno, T., 1966: Quasi-geostrophic motions in the equatorial area. *J. Meteor. Soc. Japan*, **44**, 25–43.

Petersen, W. A., R. Cifelli, D. J. Boccippio, S. A. Rutledge, and C. Fairall, 2003: Convection and easterly wave structures observed in the eastern Pacific warm pool during EPIC-2001. *J. Atmos. Sci.*, **60**, 1754–1773.

Rozendaal, M. A., and W. B. Rossow, 2003: Characterizing some of the influences of the general circulation on subtropical marine boundary layer clouds. *J. Atmos. Sci.*, **60**, 711–728.

Serra, Y. L., and R. A. Houze Jr., 2002: Observations of variability on synoptic timescales in the east Pacific ITCZ. *J. Atmos. Sci.*, **59**, 1723–1743.

Serra, Y. L., G. N. Kiladis, and M. F. Cronin, 2008: Horizontal and vertical structure of easterly waves in the Pacific ITCZ. *J. Atmos. Sci.*, **65**, 266–1284.

Takayabu, Y. N., and T. Nitta, 1993: 3-5 day-period disturbances coupled with convection over the tropical Pacific Ocean. *J. Meteor. Soc. Japan*, **71**, 221–246.

Wheeler, M., and G. N. Kiladis, 1999: Convectively coupled equatorial waves: Analysis of clouds and temperature in the wavenumber frequency domain. *J. Atmos. Sci.*, **56**, 374–399.

Wheeler, M., G. N. Kiladis, and P. J. Webster, 2000: Large-scale dynamical field associated with convectively coupled equatorial waves. *J. Atmos. Sci.*, **57**, 613–640.

Wylie, D., B. B. Hinton, and K. Kloesel, 1989: The relationship of marine stratus clouds to wind and temperature advection. *Mon. Wea. Rev.*, **117**, 2620–2625.

Xu, H., S.-P. Xie, and Y. Wang, 2005: Subseasonal variability of the southeast Pacific stratus cloud deck. *J. Climate*, **18**, 131–142.

Yanai, M., and T. Maruyama, 1966: Stratospheric wave disturbances propagating over the equatorial Pacific. *J. Meteor. Soc. Japan*, **44**, 291– 94.

Yokoyama, C., and Y. N. Takayabu, 2012: Relationships between rain characteristics and environment. part II: Atmospheric disturbances associated with shallow convection over the eastern tropical pacific. *Mon. Wea. Rev.* doi:10.1175/MWR–D–11–002511, in press.